ARCHITECTURE CIVIL ENGINEERING ENVIRONMENT
The Silesian University of Technology
No. 1/2024

doi: 10.2478/ACEE-2024-0010

APPLICATION OF SLUDGE-BASED ADSORBENT FOR ACID RED 18 ADSORPTION

Barbara PIECZYKOLAN *

* PhD; Faculty of Energy and Environmental Engineering, The Silesian University of Technology, Konarskiego 18, 44-100 Gliwice, Poland
E-mail address: *barbara.pieczykolan@polsl.pl*

Received: 8.01.2024; Revised: 23.02.2024; Accepted: 28.02.2024

Abstract
A study was conducted on the use of excess activated sludge from a municipal wastewater treatment plant as an adsorbent in the removal of Acid Red 18. The excess sludge was thermally modified using microwave radiation. The study aimed to evaluate the possibility of using this type of waste adsorbent in the batch adsorption process to remove a selected synthetic dye. Moreover, the experiments were aimed at analyzing the adsorption kinetics and adsorption isotherms of the batch adsorption process. Experimental results showed that in the case of adsorption kinetics, a greater match with experimental results was obtained for the pseudo-second-order model. This indicates that the adsorption process was chemical in nature. In the case of adsorption isotherm analysis, it showed that the best fit to experimental results was obtained for the Langmuir, Sips, and Toth isotherm models. Thus, this indicates the occurrence of a single-layer adsorption process. The determined values of adsorption capacity based on the Langmuir, Sips, and Toth models are in the range of 71.6 mg/g–79.0 mg/g.

Keywords: **Adsorption process; Adsorption kinetics; Adsorption isotherm; Dye adsorption; Sludge-based adsorbent; Activated sludge.**

1. INTRODUCTION

Synthetic organic dyes are widely used in many areas of our life, including the paper, pharmaceutical, food, textile, plastic, textile, cosmetic industries, etc. Wastewater generated during production processes may pose a serious threat to the environment due to the possible content of harmful compounds, but also due to the amount of industrial wastewater generated. For example, the textile industry requires the use of huge amounts of water (2.1% of total industrial water consumption [1]), from which post-production wastewater is then generated. The amount of textile wastewater constitutes as much as approximately 20% of the total amount of global wastewater [2, 3].

Due to the use of dyes in production processes, wastewaters that contain dyes are also generated. Therefore, these wastewaters are usually characterized by an intense color caused by dyes. Such wastewater must be properly treated before being discharged into the natural environment. The need to treat this type of wastewater arises both for reasons of environmental protection, as well as for the protection of life and health of both aquatic organisms and humans. Colored wastewater discharged into the receiver without any treatment may cause serious disturbances in the photosynthesis process of aquatic organisms. Due to their intense color, these wastewaters reduce the penetration of sunlight into the water (by scattering and absorbing light by the dyes contained in these wastewaters). The second aspect of the need to treat colored wastewater is related to their often harmful impact on human, animal, and aquatic organisms [4–9]. Moreover, most dyes contain

aromatic rings in their molecular structure, and some of them also contain azo-bounds. Azo dyes are toxic and have carcinogenic and mutagenic effects on the organisms. Dyes containing azo-bond include Acid Red 18, which was used in the experiments described in this article. Its discharge into the environment may cause reproductive toxicity and neurobehavioral effects [10, 11]. In addition, azo dyes may cause allergies, and affect the pulmonary, neural, and cardiac systems [12].

To remove and degrade dyes, many different processes, both physicochemical and chemical, are used. There can be applied techniques consisting mainly of separating the dye from wastewater. Processes with such an effect include coagulation/flocculation [13–16], membrane separation [17–19] using nanofiltration and reverse osmosis processes, as well as adsorption using activated carbons [5, 20–24]. However, methods to chemically degrade dyes in wastewater are also used. Such processes include chemical oxidation methods [25–31], advanced oxidation processes [32–41], catalytic and photocatalytic oxidation processes [42–48].

This article presents the results of using the adsorption process to remove Acid Red 18 from an aqueous solution. Excess activated sludge from a municipal wastewater treatment plant was used as an adsorbent in these studies. The activated sludge was properly prepared to obtain the powdered form of this adsorbent. Excess sludge used in this way became the so-called waste adsorbent. This type of adsorbent is also referred to in the literature as a sludge-based-activated carbon.

2. MATERIALS AND METHODS

2.1. Dye characteristics

Dye Acid Red 18 (C.I. 16255), further referred to as AR18, was used in the study [49]. It is a dye belonging to the single-azo group. Thus, it contains in its chemical structure one N = N azo bond (Fig. 1). The Molecular formula of this dye is $C_{20}H_{11}N_2Na_3O_{10}S_3$, and its weight is 604.48 g/mol. This dye is well soluble in water. In an aqueous solution, it gives an intense red color. It is mainly used for the production and dyeing of wool, silk, and polyamide fiber, as well as in the industry for dyeing leather, paper, plastic, and wood, in the medical, cosmetic, and food industries.

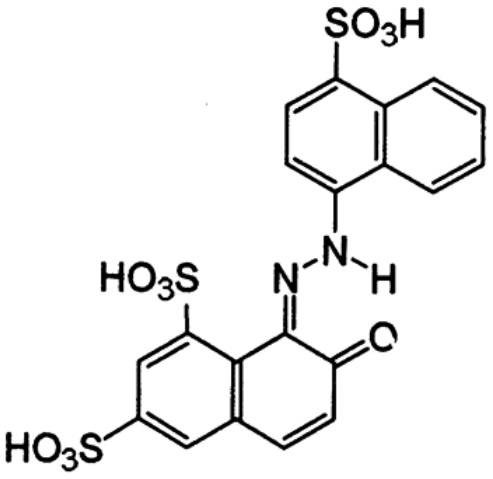

Figure 1.
Chemical structure of Acid Red 18 [49]

2.2. Preparation of an adsorbent

Excessive activated sludge from a sewage treatment plant located in southern Poland was used in the experiments. It is a treatment plant with a treatment system adapted to the removal of C, N, and P compounds by the method of aerobic activated sludge.

The excess activated sludge was collected from the secondary settling tank, then dried at 105°C, ground to a grain size < 0.49 mm, and then treated in a water bath with 700 W microwave power and a rated microwave frequency of 2450 MHz for 60 seconds for thermal activation the surface of the sludge grains. The sludge prepared in this way as a sludge-based adsorbent was used in the studies of the batch adsorption process.

2.3. Experiments' procedure

The adsorption experiments were carried out in three stages: 1) selection of the most favorable pH value for adsorption; 2) determination of the influence of contact time and determination of the adsorption kinetics; 3) determination of the adsorption isotherm and calculation of the parameters of selected models of adsorption isotherms.

To determine the most favorable pH value, the process was conducted with the use of five different pH values: 2, 4, 6, 8, and 10 while the constant values of other process conditions were used. Into the conical flask, 50 mL of the Acid Red 18 dye solution with an initial concentration of 100 mg/L was introduced, and the appropriate pH value was adjusted (by using 10% H_2SO_4 or 5% NaOH). Next 0.1 g of the sludge/sorbent was added, and the whole was mixed on a laboratory shaker for 60 minutes. After that

contact time, the adsorbent and the solution were separated, and then the final dye concentration was measured by a colorimetric method based on a standard curve at a wavelength of λ = 506 nm.

In the second stage of the studies, aimed at determining the most favorable contact time of the adsorbent and the dye, increasing contact times from 5 minutes to 180 minutes were used. During this phase of experiments, the initial concentration of the AR 18 dye was 100 mg/L and 700 mg/L, the amount of adsorbent was 0.1 g per 50 mL of the solution, and the pH of the solution was determined based on the results of the first stage of the research.

Based on the results of the influence of the contact time on the effectiveness of the adsorption process, two types of adsorption kinetics were analyzed: the pseudo-first-order (eq. 1) [50, 51] and pseudo-second-order (eq.2) [52]. To determine the parameters of each kinetics model, non-linear estimation was used – by minimizing the *RMSE* error (eq. 3). The Microsoft Office 365 Solver add-in was used in these calculations.

Equation of pseudo-first-order kinetics:

$$q_t = q_e(1 - exp(-k_1 \cdot t))[\frac{mg}{g}] \quad (1)$$

Equation of pseudo-second-order kinetics:

$$q_t = \frac{q_e^2 \cdot k_2 \cdot t}{1 + q_e \cdot k_2 \cdot t}\ [\frac{mg}{g}] \quad (2)$$

The equation for RMSE calculation:

$$RMSE = \sqrt{\frac{1}{n-2} \cdot \sum (q_{e,exp} - q_{e,calc})^2} \quad (3)$$

Where:

q_t – the amount of the dye adsorbed in a given contact time [mg/g]

q_e – the amount of the dye adsorbed at equilibrium state [mg/g]

k_1 – constant rate of a pseudo-first-order model of kinetics [/min]

k_2 – constant rate of a pseudo-second-order model of kinetics [g/(mg·min)]

t – contact time [min]

$q_{e,exp}$ – the amount of dye adsorbed obtained in the experiments [mg/g];

$q_{e,calc}$ – the amount of dye adsorbed calculated from the isotherm model or the kinetics model [mg/g].

The last, and third phases of the studies included experiments to determine the adsorption isotherm.

For this purpose, for the adjusted pH value and the contact time resulting from the second stage, increasing initial concentrations of the AR 18 dye (in the range from 100 mg/L to 1200 mg/L) were used while maintaining a constant amount of adsorbent (0.1 g per 50 mL of the dye solution).

Based on the results obtained from the third phase of the experiments, the parameters of the selected two-parameter (Langmuir [53], Freundlich [54], Jovanovic [55], Dubinin-Radushkevich [56]) and three-parameter (Sips [57] and Toth [58]) isotherm models were determined (eq. 5-12). The parameters of all examined isotherm models were determined by non-linear estimation, using the Microsoft Office 365 Solver add-in, based on the minimization of the *RMSE* error (eq. 3).

The amount of dye adsorbed per unit mass of adsorbent was calculated based on formula 4 (eq. 4).

$$q_e = \frac{(C_0 - C_e)}{m} \quad (4)$$

Where:

q_e – the amount of dye adsorbed at equilibrium state [mg/g],

C_e – concentration of the dye at equilibrium state [mg/L],

C_0 – initial dye concentration [mg/L],

m – the amount of the adsorbent [g/L].

The two-parameter isotherm models equations:

a) Freundlich model:

$$q_e = K_F \cdot C_e^{1/n} \quad (5)$$

b) Langmuir model:

$$q_e = \frac{q_m \cdot K_L \cdot C_e}{1 + K_L \cdot C_e} \quad (6)$$

c) Dubinin-Radushkevich model:

$$q_e = Q_s \cdot exp(-K_{DR} \cdot \varepsilon^2) \quad (7)$$

$$\varepsilon = RT \cdot ln\left(1 + \frac{1}{C_e}\right) \quad (8)$$

$$E = \frac{1}{\sqrt{2 \cdot K_{DR}}} \quad (9)$$

d) Jovanovic model:

$$q_e = q_{max} \cdot \left[1 - exp\left(-K_J \cdot C_e\right)\right] \quad (10)$$

The three-parameter isotherm models equations:

a) Sips model:

$$q_e = \frac{q_{mS} \cdot K_S \cdot C_e^{SP}}{1 + K_S \cdot C_e^{SP}} \quad (11)$$

b) Toth model:

$$q_e = \frac{q_{mT} \cdot K_T \cdot C_e}{(1 + (K_T \cdot C_e)^t)^{1/t}} \quad (12)$$

where:

q_e – the amount of dye adsorbed at equilibrium [mg/g],

C_e – the dye concentration at equilibrium [mg/L],

msl – the amount of the adsorbent [g/L],

K_L – Langmuir constant related to the free energy of adsorption [L/mg],

q_m – maximum adsorption capacity in Langmuir model [mg/g],

n – Freundlich equation exponents related with and adsorption intensity and heterogeneity [-],

K_F – Freundlich constant indicative of the relative adsorption capacity of the adsorbent [$mg^{(1-1/n)}L^{(1/n)}/g$],

Q_s – theoretical monolayer saturation capacity in Dubinin-Radushkevich model [mg/g],

K_{DR} – Dubinin-Radushkevich model constant [mol^2/kJ^2],

E – mean adsorption energy [kJ/mol],

ε – Polanyi potential [-],

R – gas constant [8.314 J/mol·K],

T - temperature [K],

K_J – constant related to the energy of sorption in the Jovanovic model [L/g],

q_{max} –maximum adsorption capacity in the Jovanovic model [mg/g],

q_{mS} – monolayer sorption capacity in SIPS isotherm model [mg/g],

K_S – constant in SIPS model related to the free energy of adsorption [L/mg],

SP – SIPS model exponent [-],

q_{mT} – monolayer sorption capacity in Toth isotherm model [mg/g],

K_T – constant in the Toth model related to the free energy of adsorption [L/mg],

t – Toth model exponent [-].

3. RESULTS

3.1. The effect of pH

The tests carried out in the first stage indicate that the initial pH value is extremely important for the effectiveness of the process. The tests showed that the most favorable pH value was 2.0. The use of only this reaction pH value contributed to the adsorption process and the value of the adsorbed amount of dye was 37.9 mg/g. In the case of the other higher pH values used in the tests, the adsorption process did not occur at all and the adsorbed amount of the dye was equaled 0 mg/g. Thus, no dye molecules were adsorbed on the adsorbent surface in such process conditions. The results of these tests may indicate that the surface charge of the tested adsorbent is strongly negative. On the other hand, the dye used in the tests in the hydrolysis process also acquires a negative charge. Therefore, it is necessary to use a strongly acidic condition of the adsorption process (very low pH value) and to introduce a significant excess of H^+ ions into the reaction medium. In this case, this excess of H^+ ions causes the phenomenon of protonation of the adsorbent surface and then the adsorbent surface acquires a positive charge, thanks to which it is possible to adsorb negatively charged AR 18 dye molecules on the surface.

Acid Red 18 dye adsorption studies conducted by dos Reis et al. [59] using biochar derived from birch trees wastes also showed that the adsorption efficiency decreased with increasing value of pH. A similar effect of the initial pH value of the solution on the adsorption efficiency was obtained in tests using activated carbons prepared from walnut and polar woods [60]. Also in this case, an increase in the pH value resulted in a decrease in the effectiveness of the amount of adsorbed Acid Red 18 dye on the surface of the adsorbents. Studies conducted by Pieczykolan and Płonka [61] using dried post-coagulation sludge as an adsorbent also showed that strongly acidic conditions were required for the effective adsorption of AR18 dye, and an increase in the pH value caused a drastic decrease in the efficiency of the process. The same effect of pH value was also obtained in a study of Pieczykolan and Płonka when dried and crushed excess activated sludge from a municipal wastewater treatment plant was used as an adsorbent to remove AR18 [62].

3.2. The effect of contact time

The tests to determine the effect of the contact time of the adsorbent with the dye solution were carried out at a pH of 2.0 (based on the results obtained in

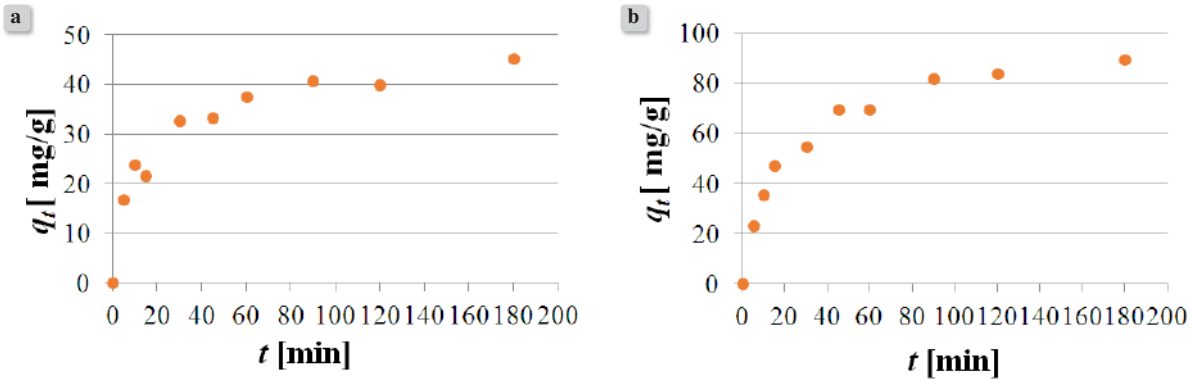

Figure 2.
The effect of contact time on adsorption efficiency: a) C_0 = 100 mg/L, b) C_0 = 700 mg/L

the first stage), the amount of adsorbent was 2 g/L and two different initial dye concentrations were used: 100 mg/L and 700 mg/L. The obtained results show that in the case of both initial concentrations, the process was the fastest during the first 20 minutes (the greatest increase in the value of the adsorbed amount of the dye q_t was observed). In the next 70 minutes, the adsorption process proceeded at a smaller speed. On the other hand, from the 90th minute, the stabilization of the q_t value was observed, which meant that the adsorption equilibrium probably has been reached. Thus, further extending the contact time of the adsorbent with the dye did not result in increasing the value of the adsorbed amount of the dye (Fig. 2).

3.3. Adsorption kinetics

Based on the results of the influence of the contact time of the adsorbent and the dye on the adsorption efficiency, the parameters of pseudo-first-order and pseudo-second-order kinetics were determined using non-linear estimation.

The conducted calculations indicate that for both tested initial concentrations of the dye, a higher degree of fit of the pseudo-second-order kinetics model to the experimental results was obtained. This is evidenced by the calculated *RMSE* error as well as the R^2 value. In the case of pseudo-second-order kinetics, the R^2 value was in the range of 0.973–0.986. However, for pseudo-first-order kinetics, it was from 0.851–0.911. Also, the calculated q_e values based on the pseudo-second-order model were more similar to the values obtained as a result of the experiments – Table 1. Better matching of the pseudo-second-order kinetics model to the experiments' results proves that in the case of the tested adsorbent-dye system, the process of chemical adsorption took place [63, 64].

Similar results of the analysis of the AR18 adsorption kinetics process were obtained in studies conducted by Shabandokht et al. when a polyaniline-modified rice husk composite was used [65].

At that time, the pseudo-second-order kinetics model also proved to be the best match to the studies' results.

However, in the case of the use of activated carbons prepared from walnut and poplar woods as adsorbents for the adsorption of AR18 by Heibati et al. [60], a better fit of the pseudo-first-order kinetics model was obtained, which indicates that physical rather than chemical adsorption occurs.

Table 1.
The parameters of kinetics models

Kinetics model	Parameter	100 mg/L	700 mg/L
Pseudo-first-order	q_e	38.5	78.0
	k_1	0.1114	0.0684
	$\boldsymbol{R^2}$	0.851	0.911
	RMSE	**0.70**	**1.03**
Pseudo-second-order	q_e	43.8	93.6
	k_2	0.0028	0.00070
	$\boldsymbol{R^2}$	0.973	0.986
	RMSE	**0.29**	**0.41**

3.4. Adsorption isotherms

The determination of the adsorption isotherm was carried out with the use of the following process parameters: initial pH of 2.0, contact time of 90 minutes, adsorbent concentration of 2 g/L, and variable initial concentration of dye in the range of 100–1200 mg/L. Based on the obtained results of these experiments, the dependence expressed by equation $q_e = f(C_e)$ was plotted (graph of the adsorption isotherm). The shape of the adsorption isotherm indicates the presence of type I adsorption by the IUPAC classification (Fig. 3). This type of adsorption curve indicates adsorption occurring in the case of microporous adsorbents with a relatively small specific surface. This type of isotherm curve is also referred to as the Langmuir isotherm which characterizes single-layer adsorption.

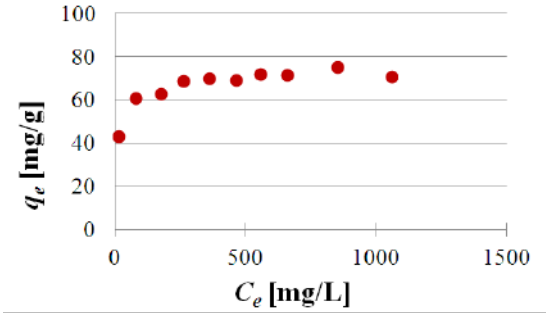

Figure 3.
Adsorption isotherm

The results of the estimation showed that in the case of two-parameter models, the greatest fit to the experimental results was obtained for the Langmuir isotherm – the determined value of the correlation coefficient R^2 was 0.928. The smallest degree of fit of the model to the study results was noted in the case of the Jovanovic model ($R^2 = 0.796$). However, in the case of three-parameter isotherm models, the best fit was obtained for the Sips and Toth isotherms – the value of R^2 was 0.967.

The calculated values of the q_m parameters of the isotherm models made it possible to determine the sorption capacity of the adsorbent for the dye AR18, the adsorption energy, and the degree of heterogeneity of the adsorbent surface.

The calculated values of the qm parameter based on the Langmuir model indicate that the sorption capacity of the monolayer is 71.6 mg/g. A similar value of the sorption capacity (in the range of 69.0–69.1 mg/g) was calculated based on the Dubinin-Radushkevich and Jovanovic isotherm models.

In the case of adsorption capacity calculated based on the SIPS model and Toth model, the value of this parameter was slightly higher – 78.1 mg/g and 79.0 mg/g for the Sips model and Toth models, respectively (Table 2).

The value of the adsorption energy calculated based on the KDR parameter of the Dubinin-Radushkevich isotherm model is 0.17 kJ/mol and indicates that physical adsorption took place in the process.

In this case, the main forces that bind the dye molecules to the adsorbent surface are the van der Waals forces.

In Langmuir, Jovanovic, Sips, and Toth isotherms models, the K_L, K_J, K_S, and K_t constants are related to the energy of the adsorption process [66–68] and the degree of affinity of adsorbate molecules to the adsorbent surface [69]. The greater the value of these

Table 2.
The parameters of sorption isotherm models

Isotherm model	Parameter	Unit	Values of parameters
Freundlich	$1/n$	-	0.108
	K_F	$mg^{(1-1/n)}L^{(1/n)}/g$	35.89
	R^2	-	0.892
	RMSE	-	3.23
Langmuir	q_m	mg/g	71.6
	K_L	L/mg	0.0944
	R^2	-	**0.928**
	RMSE	-	**2.64**
Jovanovic	q_{max}	mg/g	69.0
	K_J	L/g	0.0666
	R^2	-	0.796
	RMSE	-	4.44
Dubinin-Radushkevich	Q_S	mg/g	69.0
	KDR	mol^2/kJ^2	17.77
	E	kJ/mol	0.17
	R^2	-	0.815
	RMSE	-	4.20
Sips	q_{mS}	mg/g	78.1
	K_S	L/mg	0.2675
	SP	-	0.572
	R^2	-	**0.967**
	RMSE	-	**1.78**
Toth	q_{mT}	mg/g	79.0
	K_T	L/mg	0.5054
	t	-	0.510
	R^2	-	**0.967**
	RMSE	-	**1.78**

parameters, the greater the adsorption energy and the stronger the degree of affinity. On the other hand, the higher the degree of affinity, the stronger the adsorbate molecules are bound to the adsorbent surface. In the case of the conducted experiments in the case of the Sips model and Toth model, relatively high values of K_S and K_t were obtained, which may indicate a fairly strong bond between the dye molecules and the adsorbent surface. This fact may also be indicated by a greater adjustment of the pseudo-second-order adsorption kinetics.

The values of the *SP* parameter (exponent in Sips isotherm model), *t* parameter (exponent in Toth isotherm model), and 1/*n* parameter (constant in Freundlich isotherm model) indicate the heterogeneity, i.e. the energetic differentiation of the adsorbent surface [70]. In general, the lower the value of these parameters, the greater the surface heterogeneity. However, if the values of *SP* and *t* reach the value of 1, then the adsorbent is characterized by a homogeneous surface. When analyzing the parameters *SP* and *t* obtained as a result of the estimation, it can be noticed that their values are close to 0.5.

Thus, the surface of the tested adsorbent is characterized by a heterogeneous surface. This is also evidenced by the Freundlich model constant 1/*n*, the value of which is much lower than 1 and was rather close to 0 (Tab. 2).

The adsorption capacity results obtained in the described studies are at a comparable level to the adsorption capacity values obtained in the studies conducted by Shabandokht et al. [65] where polyaniline-modified rice husk composite was used as an adsorbent. Then the q_m value ranged from 76.92 to 100.00 mg/g depending on the type of linear estimation. However, in the research conducted by Heibati et al. [60] using activated carbon derived from poplar and activated carbon derived from walnut woods, the adsorption capacity values were lower than in the experiments described in this article. In Heibati's research, q_m values of 30.3 mg/g and 3.91 mg/g were obtained for activated carbon prepared from poplar and activated carbon prepared from walnut woods, respectively. In the case of Pieczykolan and Płonka's studies [61] using dried and crushed post-coagulation sludge to remove AR18, the adsorption capacity value was 82.2 mg/g. In contrast, when dried excess activated sludge was used (Pieczykolan and Płonka [62]) the adsorption capacity was 109.9 mg/g.

4. SUMMARY

The tests carried out on the adsorption of the Acid Red 18 dye on the sludge-based adsorbent, which was excessive activated sludge modified with electromagnetic waves, showed that:

a) the most favorable pH value of the solution for the tested dye-adsorbent system is 2; the use of a higher pH value contributed to a sharp decrease in the efficiency of the process and even the disappearance of adsorption ($q = 0$ mg/L);

b) the adsorption proceeded the fastest in the first 20 minutes of the process – the greatest increase in the value of the adsorbed amount of the AR18 was then observed. In the next 70 minutes, a further increase in qt was observed, however, it was much smaller than in the first 20 minutes, and after 90 minutes the equilibrium state of the system was achieved, after which the value of the adsorbed amount of AR18 remained at a similar level;

c) the results of the analysis of two models of adsorption kinetics indicate a better fit of the pseudo-second-order model to the experimental results – a higher value of the R^2 coefficient was obtained, and the calculated qe value based on this model is more similar to the experimental qe value; a better fit of the pseudo-second-order kinetics model indicates the chemical nature of the adsorption process;

d) the shape of the adsorption isotherm diagram is similar to the type I isotherm (according to the IUPAC classification), which indicates that single-layer sorption occurs on the microporous adsorbent;

e) the results of nonlinear estimation show that the best fit to the experimental results was obtained for the Sips and Toth models – this suggests the occurrence of single-layer adsorption;

f) the maximum adsorption capacity of the monolayer determined from the Langmuir isotherm model is 71.0 mg/g;

g) adsorption capacity estimated from the Sips and the Toth models is 78.1 mg/g and 79.0 mg/g, respectively;

h) the surface of the adsorbent is characterized by medium heterogeneity, as evidenced by the values of the parameters *SP, t*, and 1/*n*.

ACKNOWLEDGEMENTS

This work was supported by the Ministry of Education and Science Republic of Poland with statutory funds.

REFERENCES

[1] Nidheesh, P. V., Divyapriya, G., Ezzahra Titchou, F., & Hamdani, M. (2022). Treatment of textile wastewater by sulfate radical based advanced oxidation processes. *Separation and Purification Technology, 293*(April), 121115.

[2] Ma, Z., Chang, H., Liang, Y., Meng, Y., Ren, L., & Liang, H. (2024). Research progress and trends on state-of-the-art membrane technologies in textile wastewater treatment. *Separation and Purification Technology, 333*(November 2023), 125853.

[3] Mishra, V., Mudgal, N., Rawat, D., Poria, P., Mukherjee, P., Sharma, U., … Sharma, R. S. (2023). Integrating microalgae into textile wastewater treatment processes: Advancements and opportunities. *Journal of Water Process Engineering, 55*(May), 104128.

[4] Islam, A., Teo, S. H., Taufiq-Yap, Y. H., Ng, C. H., Vo, D. V. N., Ibrahim, M. L., … Awual, M. R. (2021). Step towards the sustainable toxic dyes and heavy metals removal and recycling from aqueous solution- A comprehensive review. *Resources, Conservation and Recycling, 175*(August), 105849.

[5] Yagub, M. T., Sen, T. K., Afroze, S., & Ang, H. M. (2014). Dye and its removal from aqueous solution by adsorption: *A review. Advances in Colloid and Interface Science*, 209, 172–184.

[6] Champagne, P. P., & Ramsay, J. A. (2010). Dye decolorization and detoxification by laccase immobilized on porous glass beads. *Bioresource Technology, 101*(7), 2230–2235.

[7] Weldegebrieal, G. K. (2020). Synthesis method, antibacterial and photocatalytic activity of ZnO nanoparticles for azo dyes in wastewater treatment: A review. *Inorganic Chemistry Communications, 120*(June), 108140.

[8] Carmen, Z., & Daniel, S. (2012). Textile Organic Dyes – Characteristics, Polluting Effects and Separation/Elimination Procedures from Industrial Effluents – A Critical Overview. *Organic Pollutants Ten Years After the Stockholm Convention – Environmental and Analytical Update, 2741*(31).

[9] Zhou, Y., Lu, J., Zhou, Y., & Liu, Y. (2019). Recent advances for dyes removal using novel adsorbents: A review. *Environmental Pollution*, 252, 352–365.

[10] Shokoohi, R., Vatanpoor, V., Zarrabi, M., & Vatani, A. (2010). Adsorption of acid red 18 (AR18) by activated carbon from poplar wood - A kinetic and equilibrium study. *E-Journal of Chemistry, 7*(1), 65–72.

[11] Chen, Y., Long, W., & Xu, H. (2019). Efficient removal of Acid Red 18 from aqueous solution by in-situ polymerization of polypyrrole-chitosan composites. *Journal of Molecular Liquids*, 287, 110888.

[12] Amin, M. S. A., Stüber, F., Giralt, J., Fortuny, A., Fabregat, A., & Font, J. (2023). Compact tubular carbon-based membrane bioreactors for the anaerobic decolorization of azo dyes. *Journal of Environmental Chemical Engineering, 11*(5), 110633.

[13] Zahrim, A. Y., & Hilal, N. (2013). Treatment of highly concentrated dye solution by coagulation/flocculation-sand filtration and nanofiltration. *Water Resources and Industry*, 3, 23–34.

[14] Li, H., Liu, S., Zhao, J., & Feng, N. (2016). Removal of reactive dyes from wastewater assisted with kaolin clay by magnesium hydroxide coagulation process. *Colloids and Surfaces A: Physicochemical and Engineering Aspects*, 494, 222–227.

[15] Riera-Torres, M., Gutiérrez-Bouzán, C., & Crespi, M. (2010). Combination of coagulation-flocculation and nanofiltration techniques for dye removal and water reuse in textile effluents. *Desalination, 252*(1–3), 53–59.

[16] Sultana, H., Usman, M., & Farooqi, Z. H. (2021). Micellar flocculation for the treatment of synthetic dyestuff effluent: Kinetic, thermodynamic and mechanistic insights. *Journal of Molecular Liquids*, 344, 117964.

[17] Suksaroj, C., Héran, M., Allègre, C., & Persin, F. (2005). Treatment of textile plant effluent by nanofiltration and/or reverse osmosis for water reuse. *Desalination, 178*(1-3 SPEC. ISS.), 333–341.

[18] Nataraj, S. K., Hosamani, K. M., & Aminabhavi, T. M. (2009). Nanofiltration and reverse osmosis thin film composite membrane module for the removal of dye and salts from the simulated mixtures. *Desalination, 249*(1), 12–17.

[19] Tan, Y. J., Sun, L. J., Li, B. T., Zhao, X. H., Yu, T., Ikuno, N., … Hu, H. Y. (2017). Fouling characteristics and fouling control of reverse osmosis membranes for desalination of dyeing wastewater with high chemical oxygen demand. *Desalination, 419*(June), 1–7.

[20] Khokhlova, T. D., & Hien, L. T. (2007). Adsorption of dyes on activated carbon and graphitic thermal carbon black. *Moscow University Chemistry Bulletin, 62*(3), 128–131.

[21] Hadi, M., Samarghandi, M. R., & McKay, G. (2010). Equilibrium two-parameter isotherms of acid dyes sorption by activated carbons: Study of residual errors. *Chemical Engineering Journal, 160*(2), 408–416.

[22] McKay, G., Mesdaghinia, A., Nasseri, S., Hadi, M., & Solaimany Aminabad, M. (2014). Optimum isotherms of dyes sorption by activated carbon: Fractional theoretical capacity & error analysis. *Chemical Engineering Journal*, 251, 236–247.

[23] Özacar, M., & Şengil, I. A. (2002). Adsorption of acid dyes from aqueous solutions by calcined alunite and granular activated carbon. *Adsorption, 8*(4), 301–308.

[24] Kazeem, T. S., Lateef, S. A., Ganiyu, S. A., Qamaruddin, M., Tanimu, A., Sulaiman, K. O., … Alhooshani, K. (2018). Aluminium-modified activated carbon as efficient adsorbent for cleaning of cationic dye in wastewater. *Journal of Cleaner Production*, 205, 303–312.

[25] Quan, X., Luo, D., Wu, J., Li, R., Cheng, W., & Ge, shuping. (2017). Ozonation of acid red 18 wastewater using $O_3/Ca(OH)_2$ system in a micro bubble gas-liquid reactor. *Journal of Environmental Chemical Engineering, 5*(1), 283–291.

[26] Bes-Piá, A., Iborra-Clar, A., Mendoza-Roca, J. A., Iborra-Clar, M. I., & Alcaina-Miranda, M. I. (2004). Nanofiltration of biologically treated textile effluents using ozone as a pre-treatment. *Desalination, 167*(1–3), 387–392.

[27] Srinivasan, S. V., Rema, T., Chitra, K., Sri Balakameswari, K., Suthanthararajan, R., Uma Maheswari, B., … Rajamani, S. (2009). Decolourisation of leather dye by ozonation. *Desalination, 235*(1–3), 88–92.

[28] Turhan, K., & Turgut, Z. (2009). Decolorization of direct dye in textile wastewater by ozonization in a semi-batch bubble column reactor. *Desalination, 242*(1–3), 256–263.

[29] Gao, L., Zhai, Y., Ma, H., & Wang, B. (2009). Degradation of cationic dye methylene blue by ozonation assisted with kaolin. *Applied Clay Science, 46*(2), 226–229.

[30] Gültekin, I., & Ince, N. H. (2006). Degradation of aryl-azo-naphthol dyes by ultrasound, ozone and their combination: Effect of α-substituents. *Ultrasonics Sonochemistry, 13*(3), 208–214.

[31] Konsowa, A. H. (2003). Decolorization of wastewater containing direct dye by ozonation in a batch bubble column reactor. *Desalination, 158*(1–3), 233–240.

[32] Asaithambi, P., Sajjadi, B., Abdul Aziz, A. R., & Daud, W. M. A. B. W. (2017). Ozone (O_3) and sono (US) based advanced oxidation processes for the removal of color, COD and determination of electrical energy from landfill leachate. *Separation and Purification Technology*, 172, 442–449.

[33] Katsoyiannis, I. A., Canonica, S., & von Gunten, U. (2011). Efficiency and energy requirements for the transformation of organic micropollutants by ozone, O_3/H_2O_2 and UV/H_2O_2. *Water Research, 45*(13), 3811–3822.

[34] Dadban Shahamat, Y., Masihpour, M., Borghei, P., & Hoda Rahmati, S. (2022). Removal of azo red-60 dye by advanced oxidation process O_3/UV from textile wastewaters using Box-Behnken design. *Inorganic Chemistry Communications, 143*(April), 109785.

[35] Collivignarelli, M. C., Abbà, A., Carnevale Miino, M., & Damiani, S. (2019). Treatments for color removal from wastewater: State of the art. *Journal of Environmental Management, 236*(February), 727–745.

[36] Song, H., Chen, C., Zhang, H., & Huang, J. (2016). Rapid decolorization of dyes in heterogeneous Fenton-like oxidation catalyzed by Fe-incorporated Ti-HMS molecular sieves. *Journal of Environmental Chemical Engineering, 4*(1), 460–467.

[37] Gonçalves, R. G. L., Lopes, P. A., Resende, J. A., Pinto, F. G., Tronto, J., Guerreiro, M. C., … Neto, J. L. (2019). Performance of magnetite/layered double hydroxide composite for dye removal via adsorption, Fenton and photo-Fenton processes. *Applied Clay Science, 179*(May), 105152.

[38] Shi, X., Tian, A., You, J., Yang, H., Wang, Y., & Xue, X. (2018). Degradation of organic dyes by a new heterogeneous Fenton reagent – Fe_2GeS_4 nanoparticle. *Journal of Hazardous Material*s, 353, 182–189. Retrieved from https://doi.org/10.1016/j.jhazmat.2018.04.018

[39] Quadrado, R. F. N., & Fajardo, A. R. (2017). Fast decolorization of azo methyl orange via heterogeneous Fenton and Fenton-like reactions using alginate-Fe^{2+}/Fe^{3+} films as catalysts. *Carbohydrate Polymers, 177*(June), 443–450.

[40] Gu, L., Li, C., Wen, H., Zhou, P., Zhang, D., Zhu, N., & Tao, H. (2017). Facile synthesis of magnetic sludge-based carbons by using Electro-Fenton activation and its performance in dye degradation. *Bioresource Technology, 241*(2017), 391–396.

[41] Alimard, P. (2019). Fabrication and kinetic study of Nd-Ce doped Fe_3O_4-chitosan nanocomposite as catalyst in Fenton dye degradation. *Polyhedron*, 171, 98–107.

[42] Mozia, S., Tomaszewska, M., & Morawski, A. W. (2005). Photocatalytic degradation of azo-dye Acid Red 18. *Desalination, 185*(1–3), 449–456.

[43] Mozia, S., Tomaszewska, M., & Morawski, A. W. (2007). Photodegradation of azo dye Acid Red 18 in a quartz labyrinth flow reactor with immobilized TiO2 bed. *Dyes and Pigments, 75*(1), 60–66.

[44] Bessegato, G. G., Cardoso, J. C., da Silva, B. F., & Zanoni, M. V. B. (2016). Combination of photoelectrocatalysis and ozonation: A novel and powerful approach applied in Acid Yellow 1 mineralization. *Applied Catalysis B: Environmental*, 180, 161–168.

[45] Zhang, M., Gong, J., Zeng, G., Zhang, P., Song, B., Cao, W., … Huan, S. (2018). Enhanced degradation performance of organic dyes removal by bismuth vanadate-reduced graphene oxide composites under visible light radiation. *Colloids and Surfaces A: Physicochemical and Engineering Aspect*s, 559(July), 169–183.

[46] Waghchaure, R. H., Adole, V. A., & Jagdale, B. S. (2022). Photocatalytic degradation of methylene blue, rhodamine B, methyl orange and Eriochrome black T dyes by modified ZnO nanocatalysts: A concise review. *Inorganic Chemistry Communications, 143*(May), 109764.

[47] Javanbakht, V., & Mohammadian, M. (2021). Photo-assisted advanced oxidation processes for efficient removal of anionic and cationic dyes using Bentonite/TiO_2 nano-photocatalyst immobilized with silver nanoparticles. *Journal of Molecular Structure*, 1239, 130496.

[48] Du, W. N., & Chen, S. T. (2018). Photo- and chemo-catalytic oxidation of dyes in water. *Journal of Environmental Management*, 206, 507–515.

[49] DYE|WORLD DYE VARIETY Acid Red 18. (n.d.). Retrieved from http://www.worlddyevariety.com/acid-dyes/acid-red-18.html

[50] Lagergren, S. (1898). Zur theorie der sogenannten adsorption geloster stoffe. *Kungliga svenska vetenskapsakademiens. Handlingar*, 24, 1–39.

[51] Chen, X., Chen, G., Chen, L., Chen, Y., Lehmann, J., McBride, M. B., & Hay, A. G. (2011). Adsorption of copper and zinc by biochars produced from pyrolysis of hardwood and corn straw in aqueous solution. *Bioresource technology, 102*(19), 8877–8884.

[52] Ho, Y. S., & McKay, G. (1999). Pseudo-second order model for sorption processes. *Process Biochemistry, 34*(5), 451–465.

[53] Langmuir, I. (1916). The constitution and fundamental properties of solids and liquids. *Journal of the American Chemical Society, 38*(11), 2221–2295.

[54] Freundlich, H. M. F. (1906). Over the adsorption in solution. *J. Phys. Chem*, 57, 385–470.

[55] Jovanovic, D. S. (1969). Physical adsorption of gases I: Isotherms for monolayer and multilayer adsorption. *Colloid Polym. Sci.*, 235, 1203–1214.

[56] Dubinin, M. M., & Radushkevich, L. V. (1947). The Equation of the Characteristic Curve of Activated Charcoal. *Proceedings of the Academy of Sciences, Physical Chemistry Section*, 55, 331–337.

[57] Sips, R. (1948). On the Structure of a Catalyst Surface. *The Journal of Chemical Physics, 16*(5), 490–495.

[58] Tóth, J. (1971). State Equation of the Solid-Gas Interface Layers.

[59] dos Reis, G. S., Bergna, D., Grimm, A., Lima, E. C., Hu, T., Naushad, M., & Lassi, U. (2023). Preparation of highly porous nitrogen-doped biochar derived from birch tree wastes with superior dye removal performance. *Colloids and Surfaces A: Physicochemical and Engineering Aspects, 669*(February), 131493.

[60] Heibati, B., Rodriguez-Couto, S., Al-Ghouti, M. A., Asif, M., Tyagi, I., Agarwal, S., & Gupta, V. K. (2015). Kinetics and thermodynamics of enhanced adsorption of the dye AR 18 using activated carbons prepared from walnut and poplar woods. *Journal of Molecular Liquids*, 208, 99–105.

[61] Pieczykolan, B., & Płonka, I. (2019). Post-Coagulation Sludge as an Adsorbent of Dyes from Aqueous Solutions. *Ecological Chemistry and Engineering S, 26*(3), 509–520.

[62] Pieczykolan, B., & Płonka, I. (2019). Application of Excess Activated Sludge as Waste Sorbent for Dyes Removal from their Aqueous Solutions. *Ecological Chemistry and Engineering S, 26*(4), 773–784.

[63] Larous, S., & Meniai, A. H. (2016). Adsorption of Diclofenac from aqueous solution using activated carbon prepared from olive stones. *International Journal of Hydrogen Energy, 41*(24), 10380–10390.

[64] Fadzail, F., Hasan, M., Mokhtar, Z., & Ibrahim, N. (2022). Removal of naproxen using low-cost Dillenia Indica peels as an activated carbon. *Materials Today: Proceedings, 57*(3), 1108–1115.

[65] Shabandokht, M., Binaeian, E., & Tayebi, H. A. (2016). Adsorption of food dye Acid red 18 onto polyaniline-modified rice husk composite: isotherm and kinetic analysis. *Desalination and Water Treatment, 57*(57), 27638–27650.

[66] Liu, A., He, S., Zhang, J., Liu, J., & Shao, W. (2023). Preparation and characterization of novel cellulose based adsorbent with ultra-high methylene blue adsorption performance. *Materials Chemistry and Physics, 296*(September 2022), 127261.

[67] Can, N., Ömür, B. C., & Altındal, A. (2016). Modeling of heavy metal ion adsorption isotherms onto metallophthalocyanine film. *Sensors and Actuators, B: Chemical*, 237, 953–961.

[68] Dragan, E. S., & Apopei Loghin, D. F. (2013). Enhanced sorption of methylene blue from aqueous solutions by semi-IPN composite cryogels with anionically modified potato starch entrapped in PAAm matrix. *Chemical Engineering Journal*, 234, 211–222.

[69] Araújo, C. S. T., Almeida, I. L. S., Rezende, H. C., Marcionilio, S. M. L. O., Léon, J. J. L., & de Matos, T. N. (2018). Elucidation of mechanism involved in adsorption of Pb(II) onto lobeira fruit (Solanum lycocarpum) using Langmuir, Freundlich and Temkin isotherms. *Microchemical Journal*, 137, 348–354.

[70] Ullah, S., Bustam, M. A., Al-Sehemi, A. G., Assiri, M. A., Abdul Kareem, F. A., Mukhtar, A., … Gonfa, G. (2020). Influence of post-synthetic graphene oxide (GO) functionalization on the selective CO_2/CH_4 adsorption behavior of MOF-200 at different temperatures; an experimental and adsorption isotherms study. *Microporous and Mesoporous Materials, 296*(October 2019), 110002.